Particle Identification in the PHENIX Experiment at RHIC (present and future)

Edouard Kistenev (for the PHENIX Collaboration)

Brookhaven National Laboratory, Upton, NY 11973-5000, USA

Abstract. The PHENIX[1] detector at the Relativistic Heavy Ion Collider, BNL is designed to perform a broad study of A-A, p-A and p-p collisions to investigate nuclear matter under extreme conditions. The charged particle identification is currently provided for kaons and pions to a momentum of 2.4 GeV/c and protons to 5 GeV/c. These limits would be greatly extended by the now under construction Aerogel Threshold Cherenkov detector (refractive index n=1.012).

PHENIX DETECTOR

The PHENIX detector (Fig. 1) comprises two central arms centered at zero rapidity and instrumented to detect electrons, photons and charged hadrons and two forward arms which have full azimuthal coverage and instrumented to detect muons. A number of global detectors (Zero Degree Calorimeters, Beam-Beam Counters and Multiplicity-Vertex Detector) measure the start time, vertex and multiplicity of the interactions.

In PHENIX semi-inclusive charged hadron spectra are measured in the central region over the whole kinematic range using data from a drift chambers (DC) and three segmented cathode pad chambers (PC) located outside of an axial magnetic field at a radial distances in the range of 2 to 5 m from the beam axis. About 25% of the azimuthal acceptance is covered by the time of flight system which allows k/p separation to 2.4 GeV/c and proton identification to $\sim 5GeV/c$. When track momentum is known the electron identification is performed using Ring Imaging Cherenkov Counter (RICH) and the EMCal.

CHARGED PARTICLE IDENTIFICATION IN THE PHENIX CENTRAL ARMS

Time-of-Flight subsystem

The PHENIX ToF subsystem consists of 10 panels of ToF modules with dimensions of 38 cm x 200 cm, each panel houses 96 slats of 1.5 cm x 1.5 cm plastic scintillation counters (Bicron BC404) with 3/4" diameter PMT's (HAMAMATSU R3478S) attached at both ends[2, 3]. It is designed to have about 100 ps timing resolution in order to achieve p/K separation up to 2.4 GeV/c and K/p separation up to 5 GeV/c. Figure 2 shows a plot of time-of-flight as a function of the reciprocal momentum in minimum-bias

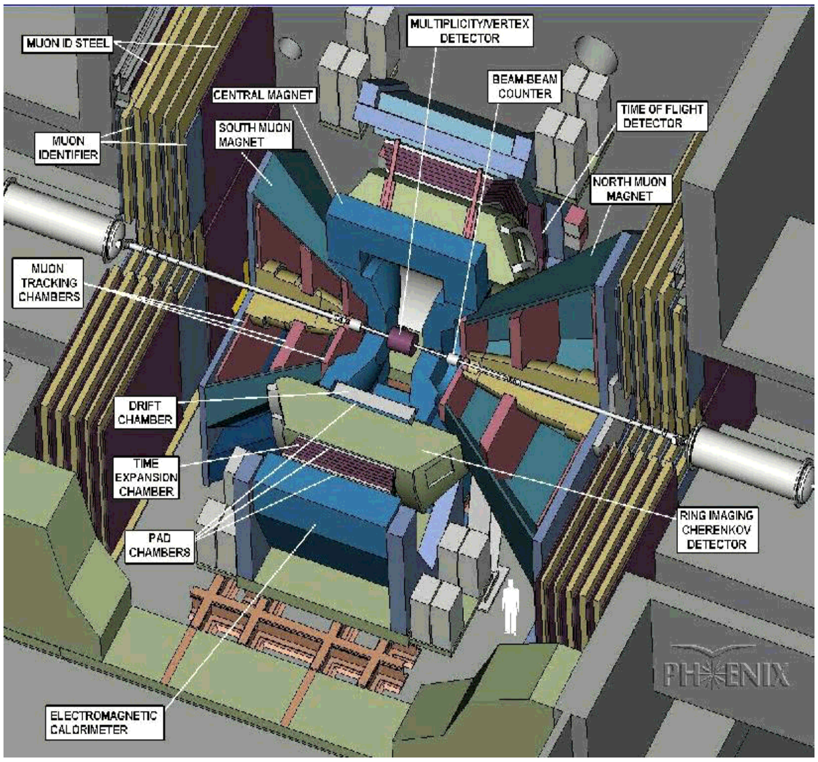

FIGURE 1. A cutaway drawing of the PHENIX detector. Labeled arrows point to the major detector subsystems.

Au-Au collisions. A resolution of $\sigma = 115ps$ was obtained in the year-1 data analysis. Ultimately, 96 ps was achieved after further calibration, as reported in [1].

Ring Imaging Cherenkov Counter

The RICH (Fig. 3) is the primary device for electron identification[4, 5, 6] in PHENIX. It is a threshold gas Cherenkov detector with a high angular segmentation to cope with the high particle density. When an electron passes through the RICH gas volume, Cherenkov photons emitted from the electron are reflected by thin spherical mirrors and are focused on arrays of PMT's, forming a ring-shaped pattern. The direction of the electron track is then measured from the position of the Cherenkov ring. A charged particle track, measured by the tracking systemn of the central arm, is identified as an electron if its direction matches the direction measured from the ring.

The e/p discrimination capabilities of the RICH are determined by the value of the pion Cherenkov threshold, the statistical fluctuations in the number of photoelectrons in the ring and the background counting rates. The best compromise between photoelectron statistics and pion threshold is reached with ethane radiator (pion threshold of 3.5 GeV/c) which has a drawback of being flammable. An alternative radiator gas which is currently used in PHENIX RICH is CO2 (pion threshold of 4.9 GeV/c). Using CO2 results in 30%

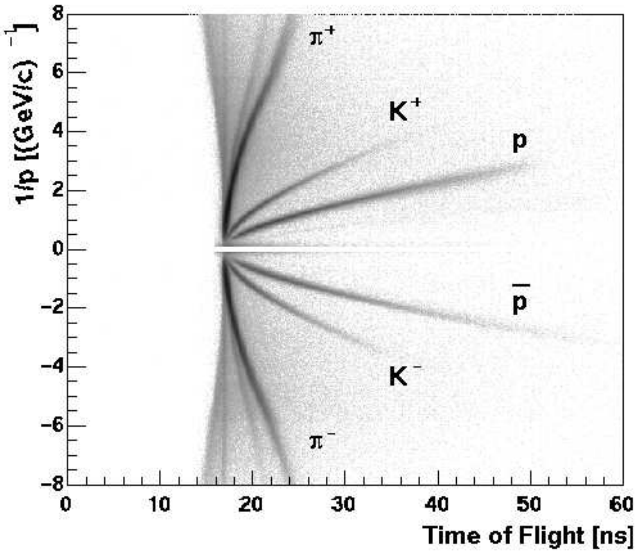

FIGURE 2. Scaled Time-of-Flight versus reciprocal momentum in minimum-bias Au+Au collisions at $\sqrt{s_{NN}}$ = 130 GeV. The distribution demonstrates the particle identification capability using the TOF for the year-1 data taking period.

light loss and decreased diameter of Cherenkov ring but has only a minimal effect on the global PHENIX electron identification capabilities which rely heavily on using different detectors in conjunction.

Electromagnetic calorimeter subsystem

The EMCal system consists of a total of 24768 individual detector modules divided between the Pb-Scintillator calorimeter which provides 75% of azimuthal coverage and Pb-glass calorimeter in the rest of the acceptance. It measures energies of the impingent electrons and photons and plays a major role in particle identification and as an important part of the PHENIX trigger system.

The electromagnetic and hadronic particles produce quite different patterns of energy sharing between calorimeter towers what allows to use measurables dependent on the shower shape to differentiate between them[1]. PHENIX calorimeters also measure particle arrival times what provides an important extra tool for particle identification. In particular, timing is the only tool to reject neutral baryons and interacting antineutrons which are a major contributor to clusters with energy $\sim 2GeV$. Slew corrected arrival times measured by exposing the calorimeter to electrons, pions and protons at 1 GeV/c momenta are shown in the top of Fig. 4. The distribution for electrons has a Gaussian shape with only a few events in the tails. The timing resolution curves (stochastic term) plotted in Fig. 4 combine the points measured by exposing the calorimeter to the particles in the 0.3-1.0 GeV/c momentum range.

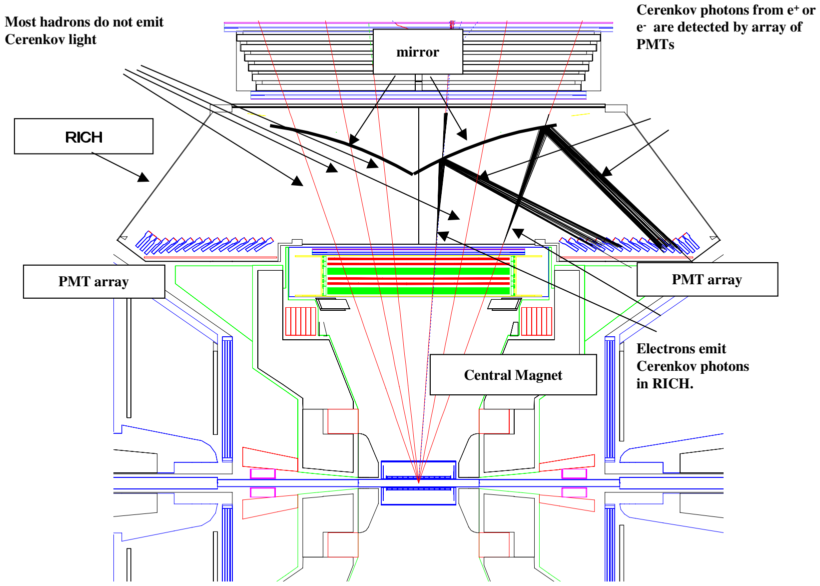

FIGURE 3. A cut-through view of PHENIX RICH detector

For energy deposits in the calorimeter $\geq 0.5 GeV$ the calorimeter timing resolution measured in the test beam is nearly constant at $\sim 120 ps$ for electrons and protons and $\sim 270 ps$ for pions where shower fluctuations are the major contributor to the measured resolution.

EXTENDED HIGH P_T HADRON IDENTIFICATION IN PHENIX

The discovery[7] of jet quenching[8] and the disappearance of back-to-back correlations[9] are the most direct evidence for the creation of dense QCD matter in nucleus-nucleus collisions. Further progress in this exiting new research program requires measuring transverse momentum spectra of identified hadron species in the transverse momentum range well above 2 GeV/c currently accessible to PHENIX. In 2001 the collaboration of PHENIX institutions began intense research and development program aimed to design, construct and install in the part of the PHENIX central Arm acceptance a new Čherenkov detector with highly segmented silica aerogel radiators. The low refractive index of the aerogel radiator makes it an ideal choice for the Cherenkov detector aimed at resolving remaining ambiguities in π/K identification

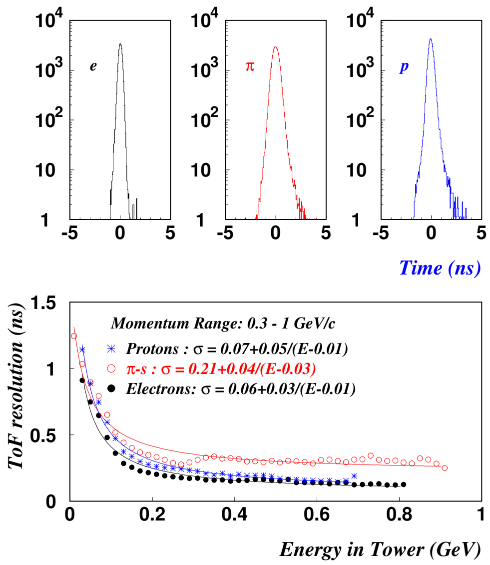

FIGURE 4. Pb-scintillator timing resolution for different particles. Top: lineshape for 1 GeV/c electrons, pions and protons. Bottom: resolution in the momentum range 0.3-1.0 GeV/c

in the few GeV/c momentum range, recent progress in manufacturing hydrophobic aerogels with improved optical quality[10] made it realistic to build and run the detector based on aerogel technology for many years without appreciable loss in the light yield.

Aerogel Detector Design

Aerogel Čerenkov detector covering the surface area of $\sim 4m^2$ will be installed into PHENIX in 2003. The detector consists of 160 identical cells of a $11 \times 22 \times 20\text{cm}^3$ packaged with aerogel (refractive index of ~ 1.011) to the half depth. An empty space in the cell is designated an integrating box which works following the priciples similar to those of "integrating sphere" used in optical measurements. Cells are built of mylar-Goretex laminate, mylar provides for the stiffness while Goretex serves as a diffuse reflector. Aerogel cells are further loaded into 0.5 mm thick Al safety and light insulating boxes, the photomultipliers attached to the box lid (see Fig. 5).

To minimize loss of the space between boxes neighboring counters have different orientation with respect to direction towards collision point - with photomultipliers upstream and downstream of the aerogel layer. The detector topology is shown in Fig.6.

Performace of the Aerogel Detector (test beam results)

A number of prototype aerogel counters differed in the refractive indices of aerogel, configuration of aerogel cells, number and location of the photomultipliers and kind

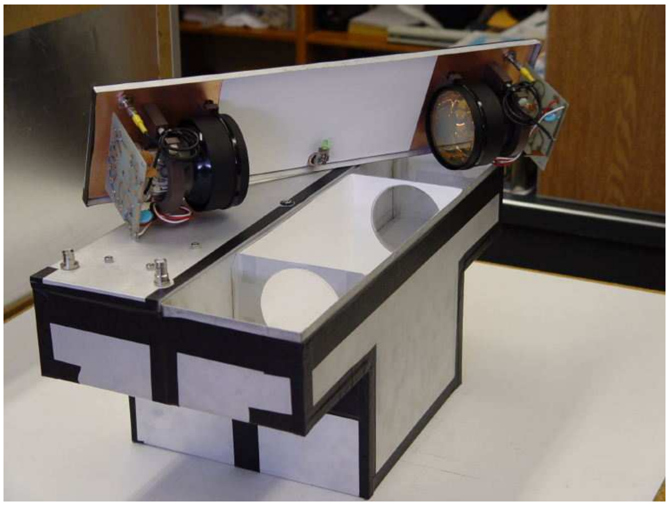

FIGURE 5. Individual aerogel box. Lid with two photomultipliers, HV bases and LED is also shown.

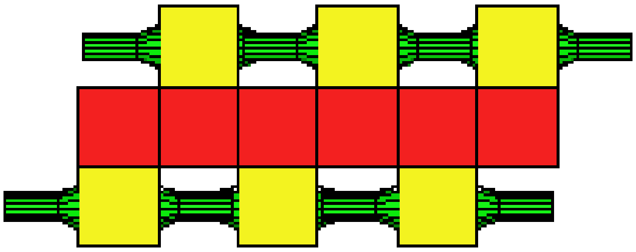

FIGURE 6. Topology of the PHENIX Aerogel Detector (view from above). Shaded - aerogel layer. PMT's viewing the neghbourring cells are upstream and downstream of the aerogel layer depending on the cell position in the layer.

of photomultipliers were tested in the test beam lines $\pi 2$ and T1 at the KEK proton synchrotron in Japan. The goal of the test beam work was to optimize the light yield and the uniformity of the light collection.

Light yield from aerogel counters

The light yield from aerogel counters was measured using cell configurations shown in the Fig.7. Block of aerogel tiles $12 \times 12 \times 12 cm^3$ in size was viewed by two 3" PMT's either in direct contact with aerogel or through the integrating box (in some cases equipped with spherical mirror). The total depth of the block (in the direction orthogonal to PMT axis) was adjustable. The refractive index of the aerogel used in this test was 1.017. The data presented below were recorded with R6233 3" HAMAMATSU

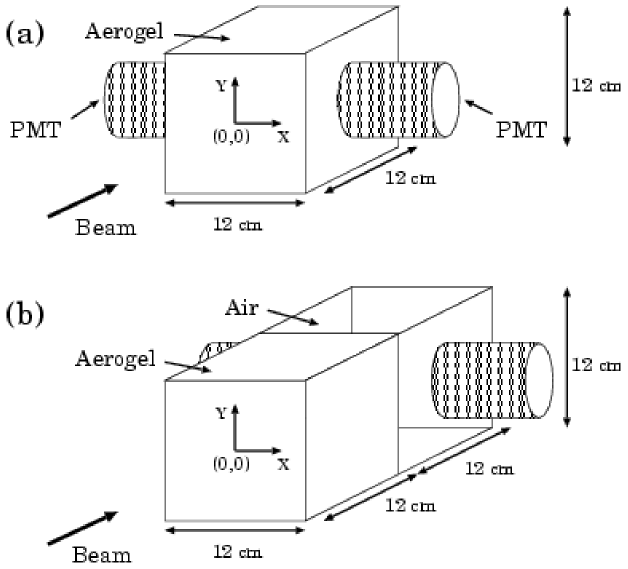

FIGURE 7. Schematic drawing of prototypes; (a)PMT's in direct contact with aerogel, (b)Light collection through integrating box.

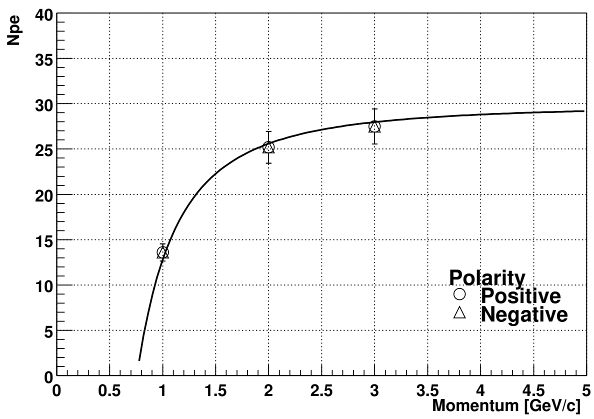

FIGURE 8. The threshold curve for pions in the n=1.017 aerogel counter. The fit as per Eq.1.

PMT's (S20 photocathode, 30% peak quantum efficiency at 420 nm). As expected(see Fig.8) the number of photoelectrons increases with the momentum, quantitatively the data agrees well with the function

$$N_{pe} \propto 1 - \frac{1}{n^2}\frac{m^2+p^2}{p^2}, \tag{1}$$

which is characteristic of the cherenkov emission.

Light yield versus the aerogel block depth is shown in Fig.9. The PMT's were either in direct contact with aerogel at the center of aerogel block (depth direction) or the distance between PMT axis and the aerogel surface was maintained equal to halfsize of the aerogel tile (6 cm). The comparison is made for the light yield measured using single PMT (morror was installed into integrating box). When block is viewed at a center line the light yield was found proportional to the total depth of the block up to the maximum depth studied of 26 cm. When light is collected through the integrating box the saturation is reached at around 13 cm depth (light is absorbed due to Rayleich scattering). We measure only 20% difference in the maximum light yield between two configuration even if the total aerogel depth is different by factor two what is consistent with nearly 100% reflectivity of Goretex.

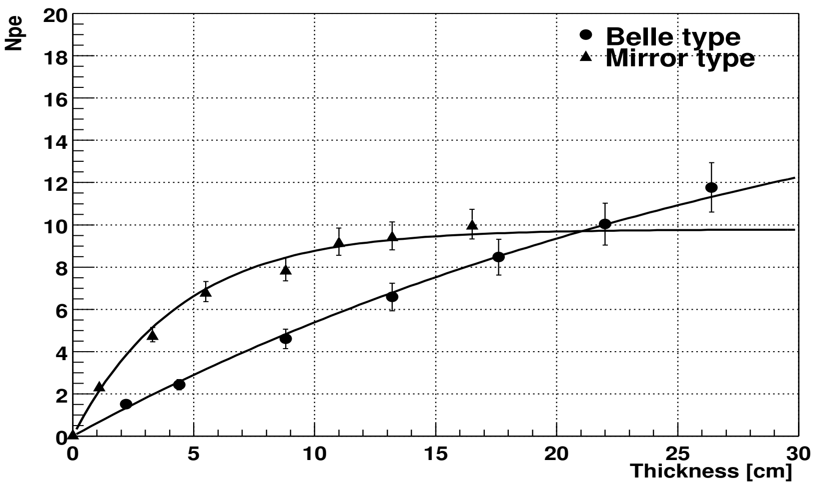

FIGURE 9. N_{pe} per PMT as a function of the aerogel block depth. Circles are for the PMT in direct contact with the block at half depth, triangles are for for mirrored integrating box. The solid curves are to guide the eyes.

The next two figures (Fig.10 and Fig.11) summarize uniformity data for the light yield in the geometry with two PMT's collecting light through the integrating box. Light yield per PMT varies for less then 30% over the whole cell surface while the total light yield stays constant to better then 15% (Fig.10). The comparison between two possible orintations (PMT's downstream or upstream) in Fig.11 shows that in the wave-length range covered by PMT's the effect of the orientation on the light yield is smaller then 30%.

The aerogel detector in PHENIX will be subjected to a very high background of secondary particles typical to heavy nuclei interractions. Only close to 5% of all charged hadrons will produce a Cherenkov light in aerogel, but a similar fraction of all charged hadrons will produce a scintillation light in the glass of the photomultiplier window. The cell design with two photomultipliers sharing in the light collection from the same cell helps to alleviate the background problem to large extent - requiring a coincidence between signals from both PMT's. An additional background rejection will be provided measuring time of the pulses from aerogel counters. Measurements made at KEK indicate that subnanosecond timing resolution can be reached triggering timing discriminator on the first photoelectron (no slewing correction). The measured dependence of the timing peak position in both PMT's on the impact point position is plotted in Fig.12

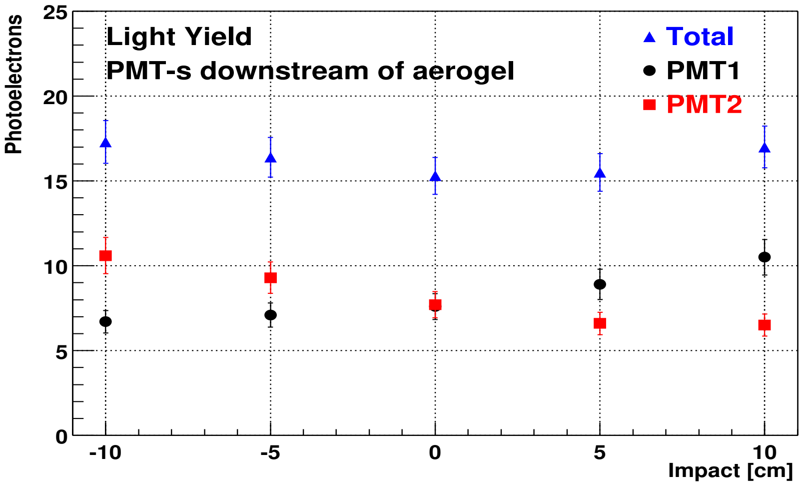

FIGURE 10. Light Yield from a single aerogel cell as a function of the impact position in the cell. Data for the cell with PMT's downstream of aerogel are shown.

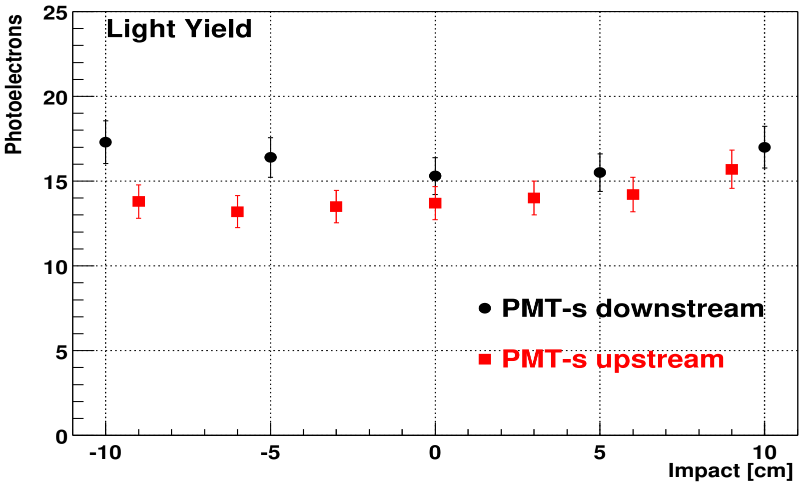

FIGURE 11. Total light yield from a single aerogel cell. Comparison is made between configurations with PMT's upstream and downstream with respect to particle direction.

A maximum timing difference 2 ns is observed between signals in two PMT's. If resolution can be improved - timing measurements in aerogel could be used for matching tracks in the spectrometer to hits in aerogel counters to better then counter size. On the other hand - if impact position is known, the appropriately corrected timing will be used to reject the soft electron background due to in flight decays.

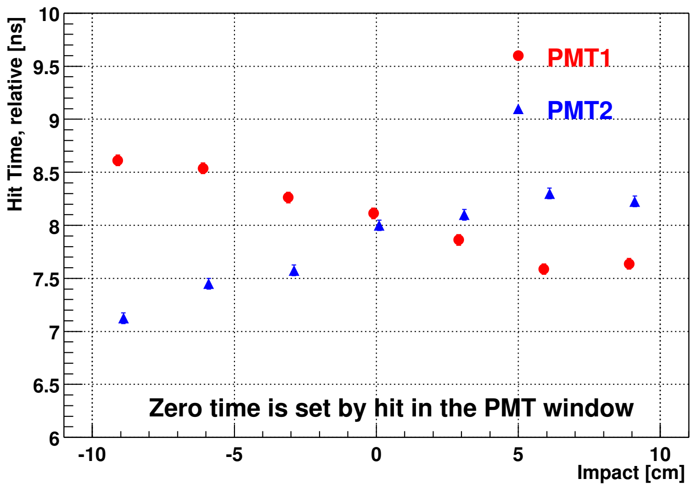

FIGURE 12. Timing difference between signals in two photomultipliers as function of the impact point position

SUMMARY

Charged hadron identification in PHENIX is performed by combining the information from DC/PC, start counters and ToF. The time-of-flight resolution of about 100 ps allows 4σ π/K separation up to $2.4GeV/c$. Upgrading the current configuration with high granularity Aerogel detector provides for the missing capability to separate π from kaons in the momentum range between 2 GeV/c and 4 GeV/c. To fully realize the potentials of this new detector PHENIX also plans to install in the same acceptance a Time-of-Flight detector with performance similar to that of described above. When project is completed the expected reach of PHENIX in identification of charged hadrons becomes complete for the whole range of kinematically accessible secondary momenta from magnetic field cutoff of $\sim 0.3GeV/c$ to nearly 17GeV/c.

REFERENCES

1. K.Adcox et al., NIM A499 (2003) 469
2. Y. Miake, American Inst. Phys. 340 (1995) 78-89
3. L.Carlen et al., NIM A431 (1999) 123-133
4. Y.Akiba et al., NIM A433 (1999) 143-148
5. Y.Akiba et al., NIM A453 (2000) 279-283
6. T.Sakaguchi et al., NIM A453 (2000) 382-385
7. K.Adcox, et al., Phys.Rev.Lett. 88 (2002) 022301
   C.Adler, et al., Phys.Rev.Lett. 89 (2002) 202301
8. P.Levai, G.Papp, G.Fai, M.Gyulassy, G.G.Barnafoldi, I.Vitev, Y.Zhang, Nucl.Phys. A698 (2002) 631
9. C.Adler, et al., nucl-ex/0206006
10. Yokogawa, Yokogawa, J.Non-Cryst. Solids 186 (1995) 23